Progress In Electromagnetics Research, PIER 79, 209–223, 2008

AN ELECTROMAGNETIC SCATTERING MODEL FOR SOYBEAN CANOPY

Y. Du, Y. L. Luo, and W. Z. Yan

The Electromagnetics Academy
Zhejiang University
Hangzhou 310058, Zhejiang, China

J. A. Kong

Department of Electrical Engineering and Computer Science
Massachusetts Institute of Technology
Cambridge, MA 02139, USA

Abstract—Extraction of vegetation water content and soil moisture from microwave observations requires development of a high fidelity scattering model. A number of factors associated with the vegetation canopy and with the underlying bare soil should be taken into account. In this paper, we propose an electromagnetic scattering model for a soybean canopy which includes the coherent effect due to the soybean structure and takes advantage of recently advanced scattering models for rough surface. We also take care of some other issues, such as including curvature effect in studying the ground bounce scattering mechanisms, and using array theory with perturbation for characterizing the inter-plant structure to account for the prevailing agriculture practice of soybean. Good agreements are obtained between the model results and measurement data.

1. INTRODUCTION

The potential use of microwave observations to monitor vegetation water content (VWC) and soil moisture is of great importance (e.g., [1–6]). Detection of VWC is useful to monitor vegetation stress and important for irrigation management and yield forecasting. Soil moisture is often the limiting factor in transpiration of plants and evaporation from soil surface, which in turn has a significant impact

on the energy cycle. Soil moisture is also a key determinant of the global carbon cycle.

Yet to extract VWC and soil moisture from microwave observations presents a big challenge, which calls for good management of many important issues, among which is the development of a high fidelity scattering model.

In developing such scattering model, a number of factors associated with the vegetation canopy and with the underlying bare soil should be taken into account. Regarding the vegetation canopy, it is important to include the coherent effect caused by the vegetation structure at low frequencies [7], an effect that has been well addressed in a number of recent models. For instance, the branching model due to Yueh et al. [8] addressed the coherence effects caused by the vegetation structure, where a two-scale branching vegetation structure was used for soybeans, and the scattered fields from constituents were added coherently. A similar treatment in considering coherent effects was proposed in [9] for forest canopies. Chiu and Sarabandi also considered the second-order, near-field interaction between constituents in addition to the coherence effect in their scattering model for soybean [10].

Yet the roughness effect of the underlying bare soil has not been adequately addressed in the above coherent models. Notarnicola and Posa, in their study of inferring VWC of corn and soybean from C- and L-band SAR images, observed that in the inversion procedure, the introduction of the dependence on roughness improves the estimates [11]. They inferred from such observation that, even for dense vegetation, the contribution from bare soil greatly influences the radar signal. To predict backscattering from the rough surface, the Kirchhoff approximation (KA) was used in [8], while a second-order small perturbation model (SPM) and a physical optic (PO) model were incorporated in [10]. It is well known that the SPM model and the KA model are applicable for slightly rough surfaces and surfaces with small surface curvatures, respectively [12, 13]. In the literature in order to bridge the gap between SPM and KA, several so-called unifying methods have been developed, including the small slope approximation (SSA) [14], the phase perturbation technique (PPT) [15], the operator expansion method (OEM) [16], the unified perturbation method (UPM) [17, 18], the full wave approach (FWA) [19, 20], the multi-scale model for exponentially correlated surfaces [21], and the integral equation method (IEM) [22]. The ability to provide good predictions for forward and backward scattering coefficients has made IEM one of the most widely used analytical models. Improvements over IEM have led to the improved IEM

model (I-IEM) [23], the advanced IEM model (AIEM) [24], the integral equation model for second-order multiple scattering (IEM2M) model [25], and most recently, the statistical IEM model (SIEM) [26] and the extended AIEM (EAIEM) model [27].

In this paper, we propose a scattering model for a soybean canopy which includes the coherent effect due to the soybean structure and takes advantage of the advanced scattering models for rough surface. We also take care of some other issues, such as including curvature effect in studying the ground bounce scattering mechanisms, and using array theory with perturbation for characterizing the inter-plant structure to account for the prevailing agriculture practice of soybean.

2. THEORETICAL MODEL

The vegetation constituents are represented by simple geometries as in [8, 10]. Specifically, stems, branches, and pods are modelled as dielectric circular cylinders of finite length. In [10] leaves are represented by elliptical thin dielectric disks, yet we found through numerical simulation that unless ellipticity ratio is much larger than unity, the final backscatter is insensitive to the ellipticity ratio, so for simplicity we model leaves as circular thin dielectric disks as in [8]. The orientation distribution of the constituents are described by two angles: the elevation angle β and the azimuth angle γ, for the latter an azimuthal symmetry is assumed.

2.1. Main Scattering Mechanisms

There are five major scattering mechanisms for a vegetation canopy: 1) direct backscatter from the underlying rough surface; 2) direct backscatter from soybean elements; 3) single ground bounce: from scatterer to ground; 4) single ground bounce: from ground to scatterer; and 5) double ground bounce. These scattering mechanisms are illustrated in Fig. 1.

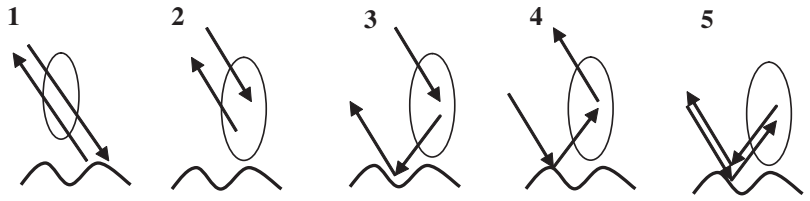

Figure 1. Major scattering mechanisms for a vegetation canopy.

Chiu and Sarabandi considered two additional scattering mechanisms [10], namely, second-order scattering interaction among vegetation constituents, and scattering interaction between main stem and the rough surface. It was concluded that the latter mechanism is only considered for predicting the cross-polarized scattering at L-band [28]. For the second-order near-field effect, good comparative illustrations with other scattering mechanisms were provided in [10] at both L- and C-band for two data sets: one from polarimetric measurements conducted using the University of Michigan polarimetric scatterometer systems (POLARSCAT) on a soybean field near Ann Arbor, MI in August 1995, when the soybean plants were fully grown with significant numbers of pods, and the other from backscatter data collected by AIRSAR during its flight over the Kellogg Biological Station near Kalamazoo, MI, on July 12, 1995, when the soybeans were about a month old. It is observed from the decomposed contributions due to different scattering mechanisms that for not fully grown soybeans (the AIRSAR data set), contribution from rough surface is at least 25 dB higher than that from the second-order interaction for co-polarized backscatter at L band, and similar observation applies to the fully grown soybeans, so the authors concluded that the contribution from the second-order near field is negligible at L-band [10]. At C-band, although the second-order near-field scattering is significant for fully grown soybeans as suggested by the authors, for not fully grown soybeans, contribution from rough surface is about 10 dB higher for the horizontally-polarized backscatter up to 50°, while showing a cross-over with the second-order interaction for the vertically-polarized backscatter at around 35°. Such observation indicates that, for not fully grown soybeans, it is more important to improve the predictive accuracy of scattering from rough surface than to include the second-order near-field effect, even at C-band, for co-polarized backscatter at small to moderate incident angles. In fact, such statement may be further strengthened if one considers the fact that the estimated ground truth in [10] corresponds to a rather smooth surface, with a rms height of 0.38 cm and a correlation length of 3.8 cm, which is several times smaller than the ground truth used in [8], where the rms height is around 1.5 cm and the correlation length is about 13 cm. The ground truth of [8] seems to agree well with other experiment studies on characterization of agricultural soil roughness for radar remote sensing [29, 30]. This suggests that the backscatter from the rough surface might be much stronger than that of [10] if ground truth comparable to that of [8, 29, 30] were to be used. Therefore, in this study, to mitigate modelling complexity we choose to apply a more rigorous treatment of the rough surface contribution using the recently advanced SIEM

model [26] but not to include the second order effect. The proposed model is expected to be useful for scattering from soybean canopy at any stage at L-band and from not fully grown soybean canopy at incident angle not very large at C-band. It can be regarded as a complementary work to that of [10].

The five scattering mechanisms are described as follows.

2.1.1. Direct Backscattering from Rough Surface

For this mechanism, we employ the recently proposed statistical multiple scattering SIEM model [26]. Unlike the conventional IEM model and its various variations, it treats the local coordinates and related field terms statistically over the orientation distribution of surface unit normal vector, which is characterized by the joint probability distribution function. Furthermore, it incorporates rigorously the shadow function in the field calculation. After some lengthy mathematical manipulation, the single- and multiple scattering coefficients of the SIEM model are obtained. For single scattering the result is

$$\sigma_{qp}^{s} = \sigma_{qp1}^{s} - \sigma_{qp2}^{s} + \sigma_{qp3}^{s} \tag{1}$$

where

$$\begin{aligned}\sigma_{qp1}^{s} &= \frac{k^2}{4\pi\cos\theta_i}\exp[-(k_{sz}+k_z)^2\sigma^2] \\ &\quad \cdot \iint\limits_{D_0} < f_{qp}(\theta_n,\phi_n) f_{qp}^{*}(\theta_n',\phi_n') > \exp[(k_{sz}+k_z)^2\psi(\rho)] \\ &\quad \cdot \exp[-i(k_{sx}-k_x)\rho\cos\phi - i(k_{sy}-k_y)\rho\sin\phi]\rho d\rho d\phi \end{aligned} \tag{2}$$

$$\begin{aligned}\sigma_{qp2}^{s} &= \frac{k^2}{2\cos\theta_i}\exp[-(k_{sz}+k_z)^2\sigma^2]| < f_{qp}(\theta_n,\phi_n) > |^2 \\ &\quad \cdot \int_0^R \rho J_0(k_{d\rho}\rho)\exp[(k_{sz}+k_z)^2\psi(\rho)]d\rho \end{aligned} \tag{3}$$

$$\begin{aligned}\sigma_{qp3}^{s} &= \frac{k^2}{2\cos\theta_i}\exp[-\sigma^2(k_z^2+k_{sz}^2)] \\ &\quad \cdot \sum_{n=1}^{\infty}\sigma^{2n}| < I_{qp}^{n} > |^2 \frac{W^{(n)}(k_{sx}-k_x, k_{sy}-k_y)}{n!} \end{aligned} \tag{4}$$

$J_0(\cdot)$ is the Bessel function of the zeroth order

$$k_{d\rho} = \sqrt{(k_{sx} - k_x)^2 + (k_{sy} - k_y)^2} \tag{5}$$

$$\begin{aligned} <I_{qp}^n> \;=\; & (k_{sz} + k_z)^n <f_{qp}> e^{-\sigma^2 k_z k_{sz}} \\ & + \frac{k_{sz}^n <F_{qp}(-k_x, -k_y)> + k_z^n <F_{qp}(-k_{sx}, -k_{sy})>}{2} \cos\theta_i \end{aligned} \tag{6}$$

$W^{(n)}(\alpha, \beta)$ is the roughness spectrum of the nth power of the surface correlation function given by

$$W^{(n)}(\alpha, \beta) = \frac{1}{2\pi} \int \psi^n(x, y) e^{-i(\alpha x + \beta y)} dx dy \tag{7}$$

Evaluation of (2) involves a six-fold integration which is quite time consuming. An approximation scheme was suggested in [26] based on a decomposition of the covariance matrix $\mathbf{C}$ into four matrices representing different types of correlation between surface norms $\hat{n}$ and $\hat{n}'$ at two points on the surface. The covariance matrix $\mathbf{C}$ is found to be

$$\begin{aligned} \mathbf{C} &= \sigma_s^2 \begin{bmatrix} 1 & 0 & \rho_{xx} & \rho_{xy} \\ 0 & 1 & \rho_{xy} & \rho_{yy} \\ \rho_{xx} & \rho_{xy} & 1 & 0 \\ \rho_{xy} & \rho_{yy} & 0 & 1 \end{bmatrix} \\ &= a\sigma_s^2 \begin{bmatrix} 1 & 0 & 0 & 0 \\ 0 & 1 & 0 & 0 \\ 0 & 0 & 1 & 0 \\ 0 & 0 & 0 & 1 \end{bmatrix} + b\sigma_s^2 \begin{bmatrix} 1 & 0 & 1 & 0 \\ 0 & 1 & 0 & 1 \\ 1 & 0 & 1 & 0 \\ 0 & 1 & 0 & 1 \end{bmatrix} \\ &\quad + c\sigma_s^2 \begin{bmatrix} 1 & 0 & 1 & 0 \\ 0 & 1 & 0 & -1 \\ 1 & 0 & 1 & 0 \\ 0 & -1 & 0 & 1 \end{bmatrix} + d\sigma_s^2 \begin{bmatrix} 1 & 0 & 0 & 1 \\ 0 & 1 & 1 & 0 \\ 0 & 1 & 1 & 0 \\ 1 & 0 & 0 & 1 \end{bmatrix} \\ &\triangleq a\mathbf{M} + b\mathbf{N} + c\mathbf{P} + d\mathbf{Q} \end{aligned} \tag{8}$$

where $b = \dfrac{\rho_{xx} + \rho_{yy}}{2}$, $c = \dfrac{\rho_{xx} - \rho_{yy}}{2}$, $d = \rho_{xy}$, and $a = 1 - b - c - d$.

The expected value of $f_{qp}(\theta_n, \phi_n) f^*_{qp}(\theta'_n, \phi'_n)$ is then expressed as

$$\begin{aligned}
& < f_{qp}(\theta_n, \phi_n) f^*_{qp}(\theta'_n, \phi'_n) > \\
= \; & (1 - |b| - |c| - |d|) \, | < f_{qp}(\theta_n, \phi_n) > |^2 \\
& + \left\{ \begin{array}{ll} b < f_{qp}(\theta_n, \phi_n) f^*_{qp}(\theta_n, \phi_n) > & (\text{if } \mathrm{b} \geq 0) \\ |b| < f_{qp}(\theta_n, \phi_n) f^*_{qp}(\theta_n, \pi + \phi_n) > & (\text{if } \mathrm{b} < 0) \end{array} \right. \\
& + \left\{ \begin{array}{ll} c < f_{qp}(\theta_n, \phi_n) f^*_{qp}(\theta_n, \frac{\pi}{2} - \phi_n) > & (\text{if } \mathrm{c} \geq 0) \\ |c| < f_{qp}(\theta_n, \phi_n) f^*_{qp}(\theta_n, \frac{3\pi}{2} - \phi_n) > & (\text{if } \mathrm{c} < 0) \end{array} \right. \\
& + \left\{ \begin{array}{ll} d < f_{qp}(\theta_n, \phi_n) f^*_{qp}(\theta_n, -\phi_n) > & (\text{if } \mathrm{d} \geq 0) \\ |d| < f_{qp}(\theta_n, \phi_n) f^*_{qp}(\theta_n, \pi - \phi_n) > & (\text{if } \mathrm{d} < 0) \end{array} \right. . \qquad (9)
\end{aligned}$$

The result for multiple scattering is

$$\begin{aligned}
\sigma^M_{qp} \; = \; & \frac{k^2}{4\pi \cos\theta_i} e^{-\sigma^2(k_z^2 + k_{sz}^2)} \sum_{n=1}^{\infty} \sum_{m=1}^{\infty} \sigma^{2n+2m} \int \{ e^{-\sigma^2 k_z k_{sz}} \\
& \cdot \left\{ \frac{[k_{sz}(k_{sz} + k_z)]^n}{n!} \frac{[k_z(k_{sz} + k_z)]^m}{m!} \mathrm{Re} < F_{qp}(u, v) >< f^*_{qp} > \right\} \\
& + \frac{k_{sz}^{2n} k_z^{2m}}{4n!m!} | < F_{qp}(u, v) > |^2 + \frac{(k_z k_{sz})^{m+n}}{4m!n!} \\
& \cdot < F_{qp}(u, v) >< F^*_{qp}(-u - k_x - k_{sx}, -v - k_y - k_{sy}) > \} \\
& \cdot W^{(n)}(k_{sx} + u, k_{sy} + v) W^{(m)}(k_x + u, k_y + v) du dv. \qquad (10)
\end{aligned}$$

All the terms in the above are referred to [26]. The results represented by (1) and (10) show that both the single and multiple scattering coefficients are similar in form to those of [22], with two distinct aspects: one, the scattering coefficients have a $\cos\theta_i$ factor in the denominators to be consistent with the conventional definition for surface scattering; and two, both f_{qp} and F_{qp} are replaced by their expected counterparts to represent their statistical characteristics.

2.1.2. Direct Backscatter from Soybean Constituents

Direct backscatter of the constituents of soybean, represented by either dielectric circular cylinders of finite length, or dielectric thin circular disks, are calculated using the generalized Rayleigh-Gans approximation [31]. This is the standard approach used in [8, 10].

2.1.3. Single and Double Ground Bounce Scattering Mechanisms

Among these two mechanisms involving ground bounce effect, the single ground bounce scatter usually contributes significantly to the

overall backscatter. As such, it requires a good characterization of the surface coherent effect. Traditional methods include directly using Fresnel reflection coefficient where the ground surface was assumed to be specular (e.g., [8]), or adding a multiplicative attenuating factor $\exp[-2(k\sigma\cos\theta)^2]$ to account for the coherent reduction caused by surface height roughness (e.g., [10]). In a study by Rodriguez [32], he observed that curvature of the surface is important as well. When a curvature related term is analytically added to the multiplicative attenuating factor, it results in an increase of the coherency as compared with otherwise. The explicit formulation that Rodriguez used to evaluate the modified Fresnel reflection coefficient is

$$R' = R_{Fresnel} \cdot \exp\left[-2(\sigma p_0)^2\left(1 + \frac{\Gamma(0)}{2p_0^2}\right)\right] v \tag{11}$$

where $R_{Fresnel}$ is the Fresnel reflection coefficient for a specular plane, $p_0 = k\cos\theta_i$ and $\Gamma(0)$ is the curvature. For a Gaussian correlated rough surface,

$$\Gamma(0) = \frac{C^{(2)}(0)}{L^2}\left(1 + \frac{1}{\cos^2\theta_i}\right) \tag{12}$$

where denotes the second derivative of correlation function. In our model we use the method similar to that of Rodriguez to evaluate the roughness modified Fresnel reflection coefficient.

2.2. Wave Propagation and Absorption in the Canopy

To evaluate the absorption and scattering effects caused by the canopy, the Foldy's approximation [1] is employed in this model, in accordance with the majority work in the literature (e.g., [8, 10]).

2.3. Scattering from Single Soybean Plant

To obtain scattering matrix of a single plant, we sum the scattering matrices of all the elements as

$$S_{pq} = S_{0pq} + \sum_{j=1}^{N_l} S_{jpq}^L + \sum_{j=1}^{N_f} S_{jpq}^F \tag{13}$$

where the subscripts p and q are unit polarizations for the incident and scattered wave, respectively. The three terms in the right side of (13) represent contributions of the stem, leaves, and fruits (if any), respectively.

2.4. Scattering from Soybean Fields

With a picture showing the top-view of soybean field at the end of the season, where all the leaves were fallen, it was suggested that the soybean plants were distributed rather randomly [10]. In [8], a hole correction approximation was used for the pair distribution function to describe the inter-plant topology. In [33], the Percus-Yevick pair distribution function was used instead. Taken into account that in typical agricultural practice plants seem to form semi-regular rows and columns, we may consider a two dimensional ground with periodically regular grids, with one plant occupying a grid yet at random position within the grid. The random departure of the plant from the center of the grid is assumed to follow a Gaussian distribution with zero mean and standard deviation, similar to the treatment in [34]. The randomness introduced this way will render a two dimensional picture (corresponding to a top-view of a field) with seemingly random placement of plants. The topology is illustrated in Fig. 2.

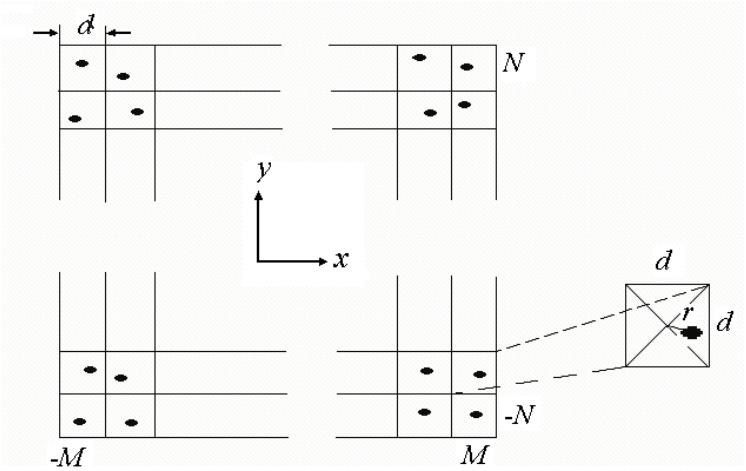

Figure 2. Inter-plant topology for a soybean canopy.

Let $S_{pq}^{(mn)}$ denote the scattering matrix from the plant in the mn-th grid ($m \in [-M, M], n \in [-N, N]$). The total scattering matrix from an aggregate of scatterers is

$$S_{pq}^{t} = \sum_{m=-M}^{M} \sum_{n=-N}^{N} S_{pq}^{(mn)}. \tag{14}$$

After some algebra, we obtain the total scattering power

$$< S_{pq}^{t} S_{pq}^{t*} > \; = \; n_s < |S_{pq}|^2 > + |< S_{pq} >|^2 \, e^{-k_{si}^2 \delta^2} \left[\left(\frac{\sin(\frac{k_x}{2})}{\sin \frac{k_x}{2\sqrt{n_s}}} \right)^2 \left(\frac{\sin(\frac{k_y}{2})}{\sin \frac{k_y}{2\sqrt{n_s}}} \right)^2 - n_s \right] \quad (15)$$

where n_s is the plant density per squared meter, and S_{pq} is the scattering matrix from a single plant given by (2).

The backscattering coefficient is defined as:

$$\sigma_{pq} = \frac{4\pi}{A_0} < S_{pq}^{t} S_{pq}^{t*} > \quad (16)$$

where A_0 is the illuminated area.

3. MODEL RESULTS AND COMPARISONS

In order to validate the proposed scattering model, we compare theoretical predictions of the polarimetric backscattering coefficients with experimental data. The data set we choose here is the same as reported in [8] to take advantage of its comprehensive ground truth. The data set covers an appreciable period of soybean growth, from

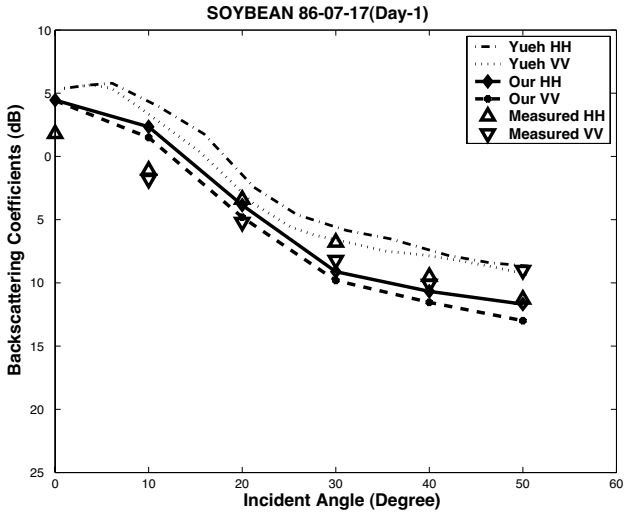

Figure 3. Comparisons between model results and measurement data.

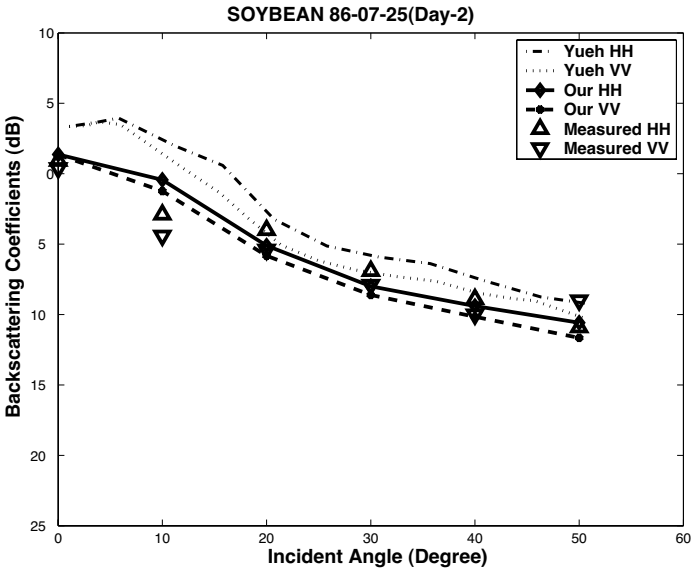

Figure 4. Comparisons between model results and measurement data.

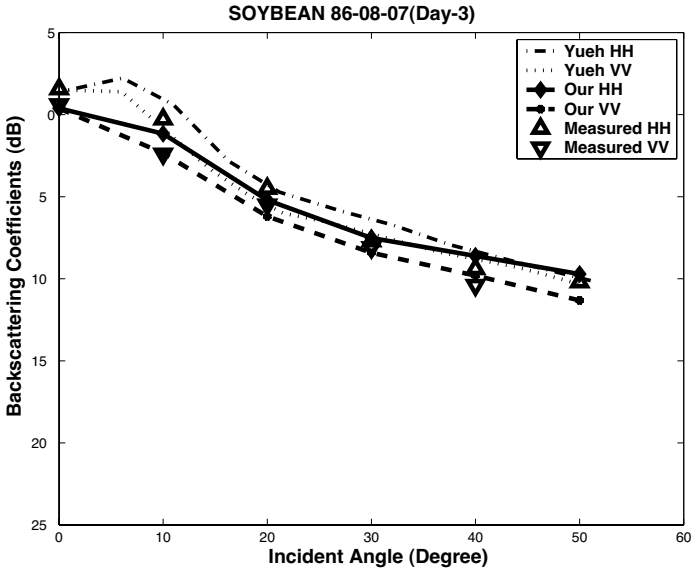

Figure 5. Comparisons between model results and measurement data.

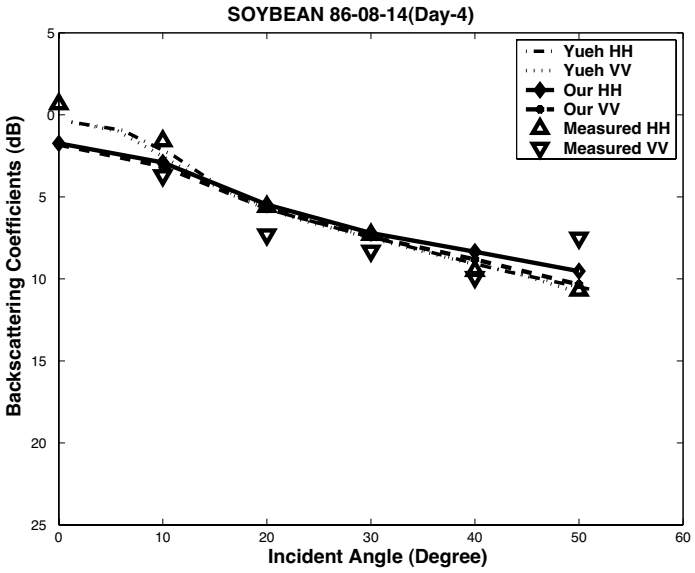

Figure 6. Comparisons between model results and measurement data.

short to fully developed plants. Fig. 3–Fig. 6 compare our theoretical results with the experimental data in four typical days of the growth period. The theoretical results obtained in [8] are also included for comparison.

One observes from the figures that both the vertically-polarized and horizontally-polarized backscattering coefficients obtained by our model are in good agreements with the experimental data. These figures also show that the proposed model outperforms the original branch model [8]. Certain overestimation of the backscattering coefficients, though less significant compared to those of [8], are observed at near normal incidence in the early days when the vegetation canopy was sparse and contribution from direct rough surface backscatter was appreciable. That is due to the carry-over effect of the overestimation by the SIEM model for rough surface scattering at near normal incidence. Addressing such discrepancy is an ongoing research.

4. CONCLUSION

In this paper, we proposed a scattering model for a soybean canopy which includes the coherent effect due to the soybean structure and takes advantage of the advanced scattering models for rough surface.

We also took care of some other issues, such as including curvature effect in studying the ground bounce scattering mechanisms, and using array theory with perturbation for characterizing the inter-plant structure to account for the prevailing agriculture practice of soybean. Good agreements were obtained between the model results and measurement data.

ACKNOWLEDGMENT

This work was supported by the National Natural Science Foundation of China (NSFC), Grant No. 40571114.

REFERENCES

1. Tsang, L., J. A. Kong, and R. T. Shin, *Theory of Microwave Remote Sensing*, Wiley-Interscience, New York, 1985.
2. Storvold, R., E. Malnes, Y. Larsen, K. A. Hogda, S. E. Hamran, K. Muller, and K. A. Langley, "SAR remote sensing of snow parameters in Norwegian areas — Current status and future perspective," *J. of Electromagn. Waves and Appl.*, Vol. 20, No. 13, 1751–1759, 2006.
3. Singh, D. and A. Kathpalia, "An efficient modeling with GA approach to retrieve soil texture, moisture and roughness from ERS-2 SAR data," *Progress In Electromagnetics Research*, PIER 77, 121–136, 2007.
4. Li, Z.-X., "Modelling the passive microwave remote sensing of wet snow," *Progress In Electromagnetics Research*, PIER 62, 143–164, 2006.
5. Mudaliar, S., "On the application of the radiative transfer approach to scattering from a random medium layer with rough boundaries," *J. of Electromagn. Waves and Appl.*, Vol. 20, No. 13, 1739–1749, 2006.
6. Arslan, A. N., J. Pulliainen, and M. Hallikainen, "Observations of L- and C-band backscatter and a semi-empirical backscattering model approach from a forest-snow-ground system," *Progress In Electromagnetics Research*, PIER 56, 263–281, 2006.
7. Zhang, G., L. Tsang, and Z. Chen, "Collective scattering effects of trees generated by stochastic Lindenmayer systems," *Microwave Opt. Technol. Lett.*, Vol. 11, 107–111, Feb. 1995.
8. Yueh, S. H., J. A. Kong, J. K. Jao, R. T. Shin, and T. Le Toan, "Branching model for vegetation," *IEEE Trans. Geosci. and Remote Sensing*, Vol. 30, No. 2, 390–401, Mar. 1992.

9. Lin, Y. C. and K. Sarabandi, "A Monte Carlo coherent scattering model for forest canopies using fractal generated trees," *IEEE Trans. Geosci. Remote Sensing*, Vol. 37, 36–40, Jan. 1997.
10. Chiu, T. and K. Sarabandi, "Electromagnetic scattering from short branching vegetation," *IEEE Trans. Geosci. and Remote Sensing*, Vol. 38, No. 2, 911–925, Mar. 2000.
11. Notarnicola, C. and F. Posa, "Inferring vegetation water content from C- and L-band SAR images," *IEEE Trans. Geosci. and Remote Sensing*, Vol. 45, No. 10, 3165–3171, Oct. 2007.
12. Kong, J. A., *Electromagnetic Wave Theory*, EMW Publishing, Cambridge, Massachusetts, 2005.
13. Ulaby, F. T., R. K. Moore, and A. K. Fung, *Microwave Remote Sensing, Active and Passive*, Vol. 2, Artech House, Norwood, MA, 1982.
14. Voronovich, A. G., "Small slope approximation in wave scattering by rough surface," *Sov. Phys. JETP*, Vol. 62, 65–70, 1985.
15. Winebrenner, D. and A. Ishimaru, "Investigation of a surface field phase perturbation technique for scattering from rough surfaces," *Radio Sci.*, Vol. 20, 161–170, Apr. 1985.
16. Milder, D. M., "An improved formalism for wave scattering from rough surfaces," *J. Acoust. Soc. Am.*, Vol. 89, 529–541, Feb. 1991.
17. Rodriguez, E. and Y. Kim, "A unified perturbation expansion for surface scattering," *Radio Sci.*, Vol. 27, 79–93, Feb. 1992.
18. Rodriguez, E., Y. Kim, and S. L. Durden, "A numerical assessment of rough surface scattering theories: Horizontal polarization," *Radio Sci.*, Vol. 27, 497–513, Aug. 1992.
19. Bahar, E., "Radio wave propagation in stratified media with nonuniform boundaries and varying electromagnetic parameters: full wave analysis," *Canad. J. Phys.*, Vol. 50, 3132–3142, 1972.
20. Bahar, E., "Radar scatter cross-sections for two-dimensional random rough surfaces: full wave solutions and comparisons with experiments," *Waves Random Media*, Vol. 6, 1–23, Jan. 1996.
21. Fung, A. K. and N. C. Kuo, "Backscattering from multi-scale and exponentially correlated surfaces," *J. of Electromagn. Waves and Appl.*, Vol. 20, No. 1, 3–11, 2006.
22. Fung, A. K., Z. Q. Li, and K. S. Chen, "Backscattering from a randomly rough dielectric surface," *IEEE Trans. Geosci. Remote Sensing*, Vol. GE-30, No. 2, 356–369, Mar. 1992.
23. Hsieh, C. Y., A. K. Fung, G. Nesti, A. Sieber, and P. Coppo, "A further study of the IEM surface scattering model," *IEEE Trans. Geosci. Remote Sensing*, Vol. 35, 901–909, May 1997.

24. Chen, K. S., T. D. Wu, L. Tsang, Q. Li, J. C. Shi, and A. K. Fung, "Emission of rough surfaces calculated by the integral equation method with comparison to three-dimensional moment method simulations," *IEEE Trans. Geosci. Remote Sensing*, Vol. GE-41, No. 1, 90–101, Jan. 2003.
25. Alvarez-Perez, J., "An extension of the IEM/IEMM surface scattering model," *Waves in Random Media*, Vol. 11, 307–329, 2001.
26. Du, Y., J. A. Kong, W. Z. Yan, Z. Y. Wang, and L. Peng, "A statistical integral equation model for shadow-corrected EM scattering from a Gaussian rough surface," *IEEE Trans. Antennas and Propag.*, Vol. 55, No. 6, 1843–1855, June 2007.
27. Du, Y., "A new bistatic model for electromagnetic scattering from randomly rough surfaces," to appear in *Waves in Random and Complex Media*.
28. Chiu, T. and K. Sarabandi, "Electromagnetic scattering interaction between a dielectric cylinder and a slightly rough surface," *IEEE Trans. Antennas Propagat.*, Vol. 47, 902–913, May 1999.
29. Davidson, M. W. J., T. L. Toan, F. Mattia, G. Satalino, T. Manninen, and M. Borgeaud, "On the characterization of agricultural soil roughness for radar remote sensing studies," *IEEE Trans. Geosci. Remote Sensing*, Vol. 38, 630–640, Mar. 2000.
30. De Roo, R. D., Y. Du, F. T. Ulaby, and M. C. A. Dobson, "Semi-empirical backscattering model at L-band and C-band for asoybean canopy with soil moisture inversion," *IEEE Trans. Geosci. Remote Sensing*, Vol. 39, No. 4, 864–872, April 2001.
31. Karam, M. A., A. K. Fung, and Y. M. M. Antar, "Electromagnetic wave scattering from some vegetation samples," *IEEE Trans. Geosci. Remote Sensing*, Vol. 26, 799–808, Nov. 1988.
32. Rodriguez, E., "Beyond the Kirchhoff approximation," *Radio Sci.*, Vol. 26, 121–132, 1991.
33. Le Toan, T., F. Ribbes, N. Floury, L. Wang, J. A. Kong, T. Kurosu, and M. Fujita, "Rice crop monitoring using ERS-1 data: Experiment and modeling results," *IEEE Trans. Geosci. Remote Sensing*, Vol. 35, 41–56, Jan. 1997.
34. Chuah, H. T., S. Tjuatja, A. K. Fung, and J. W. Bredow, "Phase matrix for a dense discrete random medium: evaluation of volume scattering coefficient," *IEEE Trans. Geosci. Remote Sensing*, Vol. 34, No. 5, 1137–1143, Sep. 1996.